Geophysical Research Letters

†These authors contributed equally to the presented work.

Key Points:
- Secondary aerosol formation studied at two sites in the atmosphere of the high Arctic
- In situ measurements observing precursor gases and further following the growth of particles up to cloud condensation nuclei sizes
- We observed significant differences of new particle formation above open ocean versus sea ice surroundings

Supporting Information:
- Supporting Information S1

Correspondence to:
M. Sipilä and L. J. Beck,
mikko.sipila@helsinki.fi;
lisa.beck@helsinki.fi

Differing Mechanisms of New Particle Formation at Two Arctic Sites

Lisa J. Beck[1,†] , Nina Sarnela[1,†] , Heikki Junninen[1,2] , Clara J. M. Hoppe[3], Olga Garmash[1] , Federico Bianchi[1] , Matthieu Riva[1,18], Clemence Rose[1,19], Otso Peräkylä[1] , Daniela Wimmer[1], Oskari Kausiala[1], Tuija Jokinen[1], Lauri Ahonen[1], Jyri Mikkilä[1], Jani Hakala[1], Xu-Cheng He[1], Jenni Kontkanen[1], Klara K. E. Wolf[3], David Cappelletti[4] , Mauro Mazzola[5] , Rita Traversi[6] , Chiara Petroselli[4], Angelo P. Viola[7], Vito Vitale[5], Robert Lange[8], Andreas Massling[8] , Jakob K. Nøjgaard[8], Radovan Krejci[9,10] , Linn Karlsson[9,10], Paul Zieger[9,10] , Sehyun Jang[11], Kitack Lee[11] , Ville Vakkari[12,13], Janne Lampilahti[1], Roseline C. Thakur[1], Katri Leino[1], Juha Kangasluoma[1,14] , Ella-Maria Duplissy[1], Erkki Siivola[1], Marjan Marbouti[1], Yee Jun Tham[1], Alfonso Saiz-Lopez[15] , Tuukka Petäjä[1], Mikael Ehn[1] , Douglas R. Worsnop[1,16], Henrik Skov[8], Markku Kulmala[1,14,17] , Veli-Matti Kerminen[1], and Mikko Sipilä[1]

[1]Institute for Atmospheric and Earth System Research/Physics, Faculty of Science, University of Helsinki, Helsinki, Finland, [2]Laboratory of Environmental Physics, Institute of Physics, University of Tartu, Tartu, Estonia, [3]Alfred-Wegener-Institut – Helmholtz-Zentrum für Polar- und Meeresforschung, Bremerhaven, Germany, [4]Department of Chemistry, Biology and Biotechnology, University of Perugia, Perugia, Italy, [5]National Research Council, Institute of Polar Sciences, Bologna, Italy, [6]Department of Chemistry, University of Florence, Florence, Italy, [7]National Research Council, Institute of Polar Sciences, Montelibretti, Italy, [8]Department of Environmental Science, iClimate, Aarhus University, Roskilde, Denmark, [9]Department of Environmental Science, Stockholm University, Stockholm, Sweden, [10]Bolin Centre for Climate Research, Stockholm University, Stockholm, Sweden, [11]Division of Environmental Science and Engineering, Pohang University of Science and Technology, Pohang, Korea, [12]Finnish Meteorological Institute, Helsinki, Finland, [13]Atmospheric Chemistry Research Group, North-West University, Potchefstroom, South Africa, [14]Beijing Advanced Innovation Center for Soft Matter Science and Engineering, Aerosol and Haze Laboratory, Beijing University of Chemical Technology, Beijing, China, [15]Department of Atmospheric Chemistry and Climate, Institute of Physical Chemistry Rocasolano, CSIC, Madrid, Spain, [16]Aerodyne Research Inc., Billerica, MA, USA, [17]Joint International Research Laboratory of Atmospheric and Earth System Sciences, Nanjing University, Nanjing, China, [18]Univ Lyon, Université Claude Bernard Lyon 1, Villeurbanne, France, [19]Laboratoire de Météorologie Physique, Aubière, France

Abstract New particle formation in the Arctic atmosphere is an important source of aerosol particles. Understanding the processes of Arctic secondary aerosol formation is crucial due to their significant impact on cloud properties and therefore Arctic amplification. We observed the molecular formation of new particles from low-volatility vapors at two Arctic sites with differing surroundings. In Svalbard, sulfuric acid (SA) and methane sulfonic acid (MSA) contribute to the formation of secondary aerosol and to some extent to cloud condensation nuclei (CCN). This occurs via ion-induced nucleation of SA and NH_3 and subsequent growth by mainly SA and MSA condensation during springtime and highly oxygenated organic molecules during summertime. By contrast, in an ice-covered region around Villum, we observed new particle formation driven by iodic acid but its concentration was insufficient to grow nucleated particles to CCN sizes. Our results provide new insight about sources and precursors of Arctic secondary aerosol particles.

Plain Language Summary Cloud properties are sensitive to the formation of new aerosol particles in the Arctic atmosphere, yet little is known about the chemistry and processes controlling this phenomenon. Here, based on comprehensive in situ measurements, we identify the very first steps of atmospheric new particle formation, that is, formation of small clusters from compounds present in the gas phase, and candidates for the subsequent growth of these clusters to larger sizes, at two Arctic sites: one surrounded by open waters, the other one by sea ice. We show how environmental differences affect secondary aerosol formation via emissions and atmospheric chemistry of aerosol precursor gases. Our results provide previously unidentified insight into how future changes in the Polar environment could

be reflected in the chain of processes linking the Arctic biosphere and cryosphere to atmospheric aerosol particles, clouds, and climate.

1. Introduction

The Polar environment is currently undergoing rapid change as manifested in decrease in snow cover (Callaghan et al., 2011), thawing of permafrost (AMAP, 2017), greening, and especially sea ice loss (Meier et al., 2014). The Arctic Ocean emits a variety of precursor gases for new particle formation (NPF) and particle growth to the sizes of cloud condensation nuclei (CCN). These gases include dimethylsulfide (DMS; Levasseur, 2013), organic compounds (Mungall et al., 2017), and iodine species (Cuevas et al., 2018; Raso et al., 2017). Coastal bird colonies form a primary source of ammonia (NH_3) in the Arctic (Croft et al., 2016) and Arctic tundra is a source of volatile organic compounds (VOC; Lindwall et al., 2016). The NPF frequency in the Arctic atmosphere was found to be correlated with the diminishing sea ice extent (Dall'Osto et al., 2017, 2018), probably via increased phytoplankton productivity, but so far the details of NPF and CCN production over ice-covered and open Arctic waters have remained largely unknown.

The absence of detailed chemical understanding down to molecular scale observations hinders estimations of the emissions of the precursor gases, or their contribution to the initial steps of NPF and subsequent particle growth (S. H. Lee et al., 2019). More importantly, those will change in response to the changing climate. Further decrease of sea ice extent may lead to enhanced open ocean phytoplankton productivity and DMS emissions (Galí et al., 2019), while increased terrestrial primary production due to warming has already caused enhanced biogenic volatile organic compound emissions (Lindwall et al., 2016) that can undergo autoxidation and lead to elevated gas-phase highly oxygenated organic molecule (HOM) concentrations (Bianchi et al., 2019; Ehn et al., 2014). Homogeneous nucleation of iodic acid (HIO_3, IA) occurs over the ice-covered Arctic Ocean (Baccarini et al., 2020; Sipilä et al., 2016), while sulfuric acid (H_2SO_4, SA, formed through oxidation of marine DMS via SO_2), NH_3, and air ionization by galactic cosmic radiation drive NPF in coastal Antarctica (Jokinen et al., 2018).

To bridge the connection between sea ice decline and associated changes in oceanic precursor emissions and related effect on aerosol and CCN populations, we conducted a suite of measurements at the two sides of the Fram Strait – at Villum Research Station, North Greenland, and at Ny-Ålesund on Svalbard. The stations are located at similar latitudes within a distance of about 600 km but they have distinctly different environmental conditions. Western Svalbard (Ny-Ålesund) is surrounded by open waters throughout the whole year due to advection of warm Atlantic water, whereas the ocean next to the North-Eastern coast of North Greenland (Villum) is permanently covered by ice with some larger polynyas occurring in the late summer.

Here we use state-of-the-art instrumentation, which enables observation of the NPF mechanism starting from molecular level and growing further to CCN sizes. Our study shows significant differences in particle formation and growth between these two locations (Figure S1) and over different seasons. We show the relevance of low-volatility vapors, such as SA together with NH_3, IA, HOM, and methane sulfonic acid (CH_3HSO_3, MSA) in Arctic NPF.

2. Materials and Methods

We conducted a measurement campaign at Villum Research Station in North Greenland (81°36′N, 16°39′W) from mid-February 2015 until the end of August 2015. At Villum, the particle number size distribution in the diameter range of 10–900 nm has been measured with a Scanning Mobility Particle Sizer (SMPS, Wang & Flagan, 1990) since 2010 (Dall'Osto et al., 2018; Nguyen et al., 2016). Additionally, we conducted a second campaign in Ny-Ålesund, Svalbard (78°55′N, 11°56′E), from the end of March 2017 until the end of August 2017. The measurements took place in the atmospheric observatory, Gruvebadet, located 2 km southeast of Ny-Ålesund.

During our measurement campaigns, we used a nitrate chemical ionization atmospheric pressure interface Time-Of-Flight mass spectrometer (CI-APi-TOF, Jokinen et al., 2012) to measure low-volatility va-
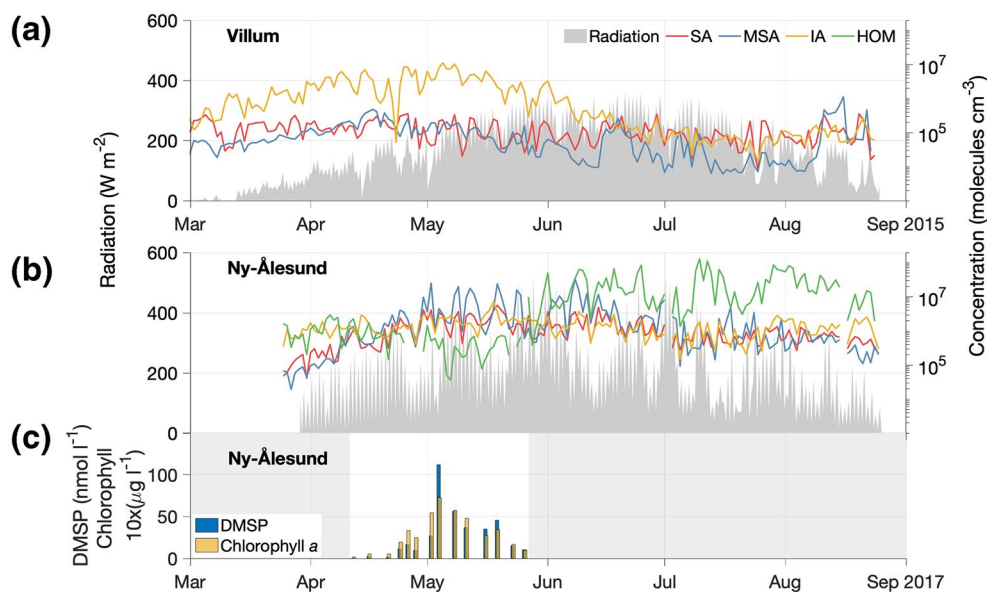
Figure 1. Daily average concentrations of marine phytoplankton indicators, precursor vapors and 6 hour average of solar radiation intensity. Measured solar radiation intensity and concentrations of sulfuric acid (SA), methane sulfonic acid (MSA), iodic acid (IA), and highly oxygenated organic molecules (HOM) (a) at Villum and (b) at Ny-Ålesund. (c) Seawater chlorophyll *a* and dimethylsulfoniopropionate (DMSP) concentrations (10 m depth) at Ny-Ålesund from April 12 to May 26, 2017.

pors, APi-TOF (Junninen et al., 2010) to measure ambient ions and clusters, and Particle Size Magnifiers (Vanhanen et al., 2011) to measure the concentration of sub-3 nm particles. At Villum, we used an Air Ion Spectrometer (AIS, Mirme & Mirme, 2013) to measure the charged particle number size distribution in the diameter range of 0.8–40 nm, and at Ny-Ålesund, we measured with a Neutral cluster and Air Ion Spectrometer (Manninen et al., 2009) which is measuring same sized charged particles as well as neutral particles (2–42 nm). Additionally, we used SMPS data, which are continuously measured at Gruvebadet. Furthermore, we measured marine chlorophyll *a* and dimethylsulfoniopropionate (DMSP) concentrations in nearby waters. The samples were collected between April 12, 2017 and May 26, 2017 at 10 m depth in Kongsfjorden, in a midfjord location in front of Ny-Ålesund.

3. Results and Discussion

3.1. Overall Behavior of Aerosol Precursor Gases

Following the end of the Polar night in February at Villum, we found a rise in the IA concentration with increasing intensity of solar radiation (Figure 1a). After the IA maximum close to 5×10^7 molecules cm^{-3} in early May, the IA concentration started to decay likely due to changes in sea ice properties and extent or ice-borne microalgae productivity (Saiz-Lopez et al., 2015). SA and MSA concentrations were rather low, and we did not detect gas-phase HOM during our campaign.

At Ny-Ålesund, the springtime IA concentration was lower and exhibited less pronounced temporal changes compared to Villum. In contrast, the concentrations of SA and MSA started to increase rapidly with an increasing radiation intensity, reaching daily average values larger than 10^6 molecules cm^{-3} for SA and larger than 10^7 molecules cm^{-3} for MSA (Figure 1b). This rise coincided with the start of the phytoplankton bloom in mid-April, observed as an increase in chlorophyll *a* concentration in seawater (Figure 1c). During the peak of the bloom in early May, highly elevated DMSP concentrations were observed. During the 2017 bloom, the dominant plankton species was observed to be *Phaeocystis pouchetii*, a strong DMSP producer (Stefels et al., 2007). The species dominance, however, may vary regionally and from year to year (Hegseth et al., 2019). The high SA and MSA concentrations prevailed throughout June, which agrees with previous
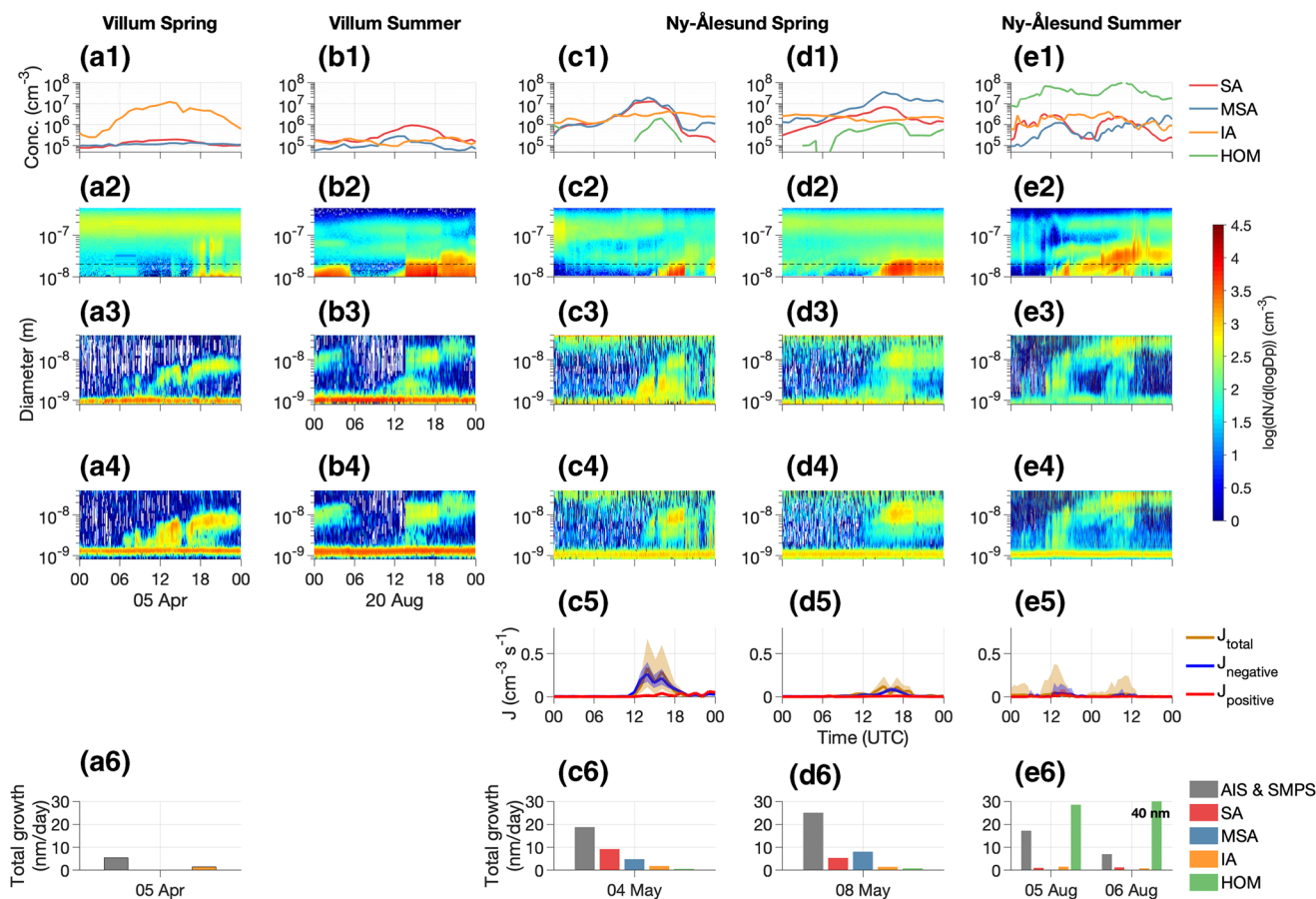
Figure 2. Examples representing seasonal behavior of NPF observed at Villum and Ny-Ålesund. The first two columns show data from Villum during spring and summer: (a) April 5, 2015, (b) August 20, 2015. Columns c to e show data from Ny-Ålesund: (c) May 4, 2017, (d) May 8, 2017, and (e) August 5–6, 2017. (a1)–(e1): SA, MSA, IA, and HOM concentrations in molecules per cm^3. (a2)–(e2): Particle size distributions with a diameter >10 nm. The dashed line shows 20 nm diameter. (a3)–(e3) and (a4)–(e4): negative and positive ion size distributions with a diameter of 0.8–40 nm, respectively. (c5)–(e5): Total, negative ion-induced and positive ion-induced nucleation rates (J) in cm^{-3} s^{-1}. Negative ion-induced nucleation drives particle formation with a contribution from positive ion-induced nucleation as well as potentially neutral nucleation during summer. The shaded area indicates the uncertainties. (a6) & (c6)–(e6): Total daily particle growth, calculated from particle measurements (AIS & SMPS), as well as based on gas concentrations of SA, IA, MSA, and HOM assuming kinetic condensation. For SA growth rate (GR), the dipole-dipole enhancement was taken into account (Halonen et al., 2019). Other GR were calculated based on Nieminen et al. (2010) due to lack of knowledge about enhancement of their collision rates.

studies of the observed phytoplankton activity in the Arctic Ocean (Assmy et al., 2017). HOM concentrations at Ny-Ålesund were very low during spring but started to increase steeply after the snow melt in the end of May (Figure S2). Due to the complexity of the spectrum and the insufficient resolution of the instrument, it was not possible to identify the elemental composition of the HOM.

3.2. Particle Formation at Ny-Ålesund and Villum

Figure 2 shows a zoom-in to five examples of NPF events with distinctly different concentrations of particle precursor vapors. At Villum, IA was the prominent driver for NPF in springtime as nucleation was associated with high concentrations of IA, while SA and MSA remained low (Figure 2a.1, Figure S3). Both negative and positive ions seemed to contribute to the particle formation (Figures 2a.3 and 2a.4). The composition of negative ion clusters (Figure 3c) could mostly be explained by IA, even though SA was found in both iodine clusters and in some of the smallest clusters either alone or together with NH_3. The particle growth, however, was dominated by IA condensation (Figure 2a.5, see also Figure S3). Particles only grew up to 10 nm in diameter or slightly above (Figure 2a.2). In summertime, IA concentrations were lower and
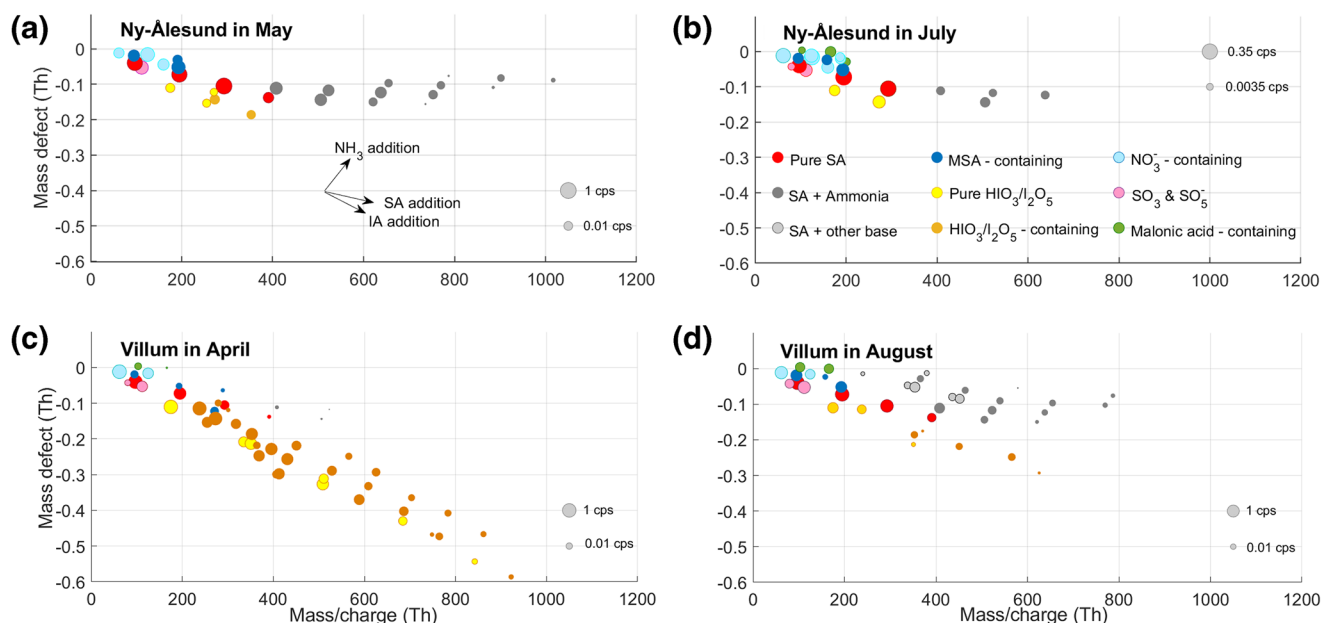
Figure 3. Mass defect plot of identified negative ion clusters during nucleation events. (a) Ny-Ålesund in May 2017 and in July 2017 (b) as well Villum in April 2015 (c), and August 2015 (d) measured with APi-TOF. Each panel shows one event representing the events of that season. The mass defect is presented versus the ion/cluster mass/charge ratio depicting the abundance and atomic composition of nucleating ion clusters. The area of the dots is logarithmically proportional to the observed signal (counts per second). At Ny-Ålesund, MSA, IA and nitrate/nitric acid are detected in some of the smallest clusters but SA-NH$_3$ nucleation is a sole pathway for new particle nucleation. In springtime Ny-Ålesund, the largest detected cluster contained 8 molecules of SA and 8 molecules of NH$_3$ on bisulfate core ion (HSO$_4^-$) formed via interactions of SA and air ions. During summertime at Ny-Ålesund, SA-NH$_3$ clusters are not as abundant anymore as in springtime. At Villum in springtime, some SA-NH$_3$ clusters are seen but the nucleation is dominated by iodic acid clusters. The majority of the IA clusters contain also SA and/or sulfur trioxide. The observed I$_2$O$_5$ clusters likely form from restructuring of two IA molecules in the clusters and recycling of water (Sipilä et al., 2016). During summertime in Greenland, there are more SA-NH$_3$ clusters abundant in the atmosphere while iodine-containing clusters are seen to less extent than in springtime.

only a few weak NPF events were observed (Figure 2b.1) while negative ion-induced nucleation seemed to initiate the clustering (Figures 2b.3 and 2b.4). The identified nucleating clusters at Villum were composed of SA and NH$_3$ (Figure 3d). At Villum, the concentrations of particles larger than 10 nm were higher during summertime compared to spring, and according to our AIS measurements, the larger particles detected by SMPS were not nucleating in the vicinity of Villum but were advected there and continued to grow on site (Figure S4). Previous studies have observed that larger, accumulation mode particles consisted mainly of sulfate and some organic material (Lange et al., 2018; Nielsen et al., 2019).

At Ny-Ålesund, the concentrations of SA and MSA were clearly higher (Figure S5). On 4 May, they peaked at about 10^7 molecules cm^{-3} (Figure 2c.1) while IA concentration showed no clear temporal behavior, and the HOM concentration was low. Associated with the high SA concentration, we observed SA-NH$_3$ ion clusters (Figure 3a), indicating a clear negative ion-induced nucleation. Simultaneously, we observed the appearance of negative ion clusters between about 1 and 3 nm (Figure 2c.3), and the formation rate of 1.5 nm negative ions ($J_{negative}$, $J_{neg,max}$ = 0.33 cm^{-3}s^{-1}) was close to that of total 1.5 nm particles (J_{total}, $J_{tot,-max}$ = 0.27 cm^{-3}s^{-1}; Figure 2c.5). The overall growth of newly formed particles to larger sizes was modest on this day, with particles reaching a maximum size of 20 nm in diameter (Figure 2c.6). During 8 May, we observed another example of negative ion-induced nucleation initiating the particle formation on both days (Figures 2d.3 and 2d.5, Figure S5), and with positive ion-induced nucleation being absent (Figures 2d.4 and 2d.5). While SA, IA, and HOM concentrations were similar to those on 4 May, the MSA concentration was higher by a factor of 5–6, leading to a higher total particle growth rate (Figure 2d.6). Pronounced growth with higher MSA was observed throughout the spring period (Figure S5). On 5 and 6 August, the HOM concentrations were two orders of magnitude higher than in the springtime (Figure 2e.1), whereas SA and MSA concentrations were low. During summertime, the early growth (1.5–3 nm) was visible similarly in

both polarities (Figures 2e.3 and 2e.4), suggesting that the dominant particle formation mechanism was different from that in spring.

Direct measurements of ion cluster composition in springtime Ny-Ålesund showed the abundance of SA and NH_3 in small negative clusters (Figure 3a), in line with the observed nucleation rates. A comparison of observed (total) formation rates of 1.5 nm particles to the parameterizations based on experimental results (Dunne et al., 2016) suggests regional springtime NH_3 concentrations of 10^8–10^9 cm^{-3} (Figure S6a) in line with a recent modeling study (Croft et al., 2016), meaning that the nucleation rate is sensitive to both SA and NH_3. Those observations align with a recent study by Giamarelou et al. (2016), indicating that 12-nm particles consist mainly of ammonium sulfate at Zeppelin Observatory in Ny-Ålesund. Furthermore, the nucleation rate is also sensitive to ion concentration and thus to the level of ionizing radiation due to the dominance of ion-induced pathway in the SA + NH_3 + H_2O system with nucleation rates below ion-pair production rate (~2 ion pairs per second) (Dunne et al., 2016; Kirkby et al., 2011). MSA and IA appeared to have only a small role in the initial stages of particle formation. However, any change in the SA, MSA, and IA concentration distribution could lead to a more complex nucleation mechanism, already reflected here as the smallest clusters containing MSA or IA (Figures 3a and 3b). The identified negative clusters during summertime events with high neutral HOM concentrations showed a similar composition, with clearly detectable SA-NH_3 clusters (Figure 3b), but unlike in springtime, malonic acid was present. Since HOM concentrations were high during summertime, it is highly probable that besides SA-NH_3 ion-induced nucleation, also (ion-induced) SA-HOM nucleation (Riccobono et al., 2014), pure biogenic (ion-induced) nucleation of HOM (Kirkby et al., 2016), and/or multicomponent SA-NH_3-HOM nucleation (Lehtipalo et al., 2018) contributed to the total particle formation rate (Figure 2e.5). HOM concentrations of just a few 10^6 molecules cm^{-3} are sufficient to promote nucleation together with SA (Riccobono et al., 2014), whereas HOM concentrations of a few 10^7 molecules cm^{-3} can initiate NPF in the absence of SA, and nucleation can be seen equally effectively with both polarities (Kirkby et al., 2016).

3.3. Particle Growth and Subsequent CCN Production

Our observations at Ny-Ålesund suggest that MSA frequently had a significant contribution to the growth of newly-formed particles (Figures 2b and S6b). This is quite a surprising result, considering that MSA is more volatile than SA (Berresheim et al., 2002), and that the observed methane sulfonate-to-non-sea-salt-sulfate ratios (MSA$^-$/nss-SO$_4^{2-}$) in the bulk summer Arctic aerosol are usually (also in our case) well below unity (L. Chen et al., 2012; Figure S7). The reason for low MSA$^-$/nss-SO$_4^{2-}$ in bulk aerosol samples is most probably associated with heterogeneous reactions producing sulfate in wet aerosol particles or cloud droplets (Pozzoli et al., 2008) more efficiently than methane sulfonate (Q. Chen et al., 2018; Hodshire et al., 2019), or with long-range transportation of anthropogenic sulfate (L. Chen et al., 2012). Thus, bulk aerosol measurements clearly do not reflect the growth mechanisms or chemical composition of the smallest particles. In chamber studies, MSA has been shown to form particles in mixtures (Dawson et al., 2012) and our observations suggest that MSA is an important component of the Arctic secondary aerosol.

During summer, the particle growth was obviously dominated by HOM condensation at Ny-Ålesund (Figure 2c.6), as the particles grew up to 40 nm in spite of low concentrations of SA, MSA, and IA. The high concentration and predominant role of HOM in the particle growth is also an unexpected result, considering that the terrestrial biomass in the Ny-Ålesund area is scarce. HOM concentrations in excess of 10^8 molecules cm^{-3} are typical for forests (Ehn et al., 2014), and therefore finding similar concentrations in Svalbard was a surprise. An explanation for this could be the very low condensation sink of $\sim 4 \times 10^{-4}$ s^{-1} at Ny-Ålesund ($\sim 3 \times 10^{-4}$ s^{-1} at Villum), which allows a more efficient buildup of the gas-phase HOM concentration tied to the slower scavenging rate of HOM by pre-existing aerosol particles.

The climatic effects of atmospheric NPF are tied closely with two issues: the growth of newly-formed particles to sizes large enough to be able to act as CCN (Gordon et al., 2017; Kerminen et al., 2012), and the susceptibility of cloud properties to additional CCN (e.g., Moore et al., 2013; Zhao et al., 2018). The susceptibility of clouds to CCN tends to be highest under clean atmospheric conditions, such as those typically observed over the Arctic outside the Arctic haze period. Cleaner conditions also tend to cause higher water vapor supersaturations inside liquid clouds (Hudson & Noble, 2014), reducing the minimum size at which
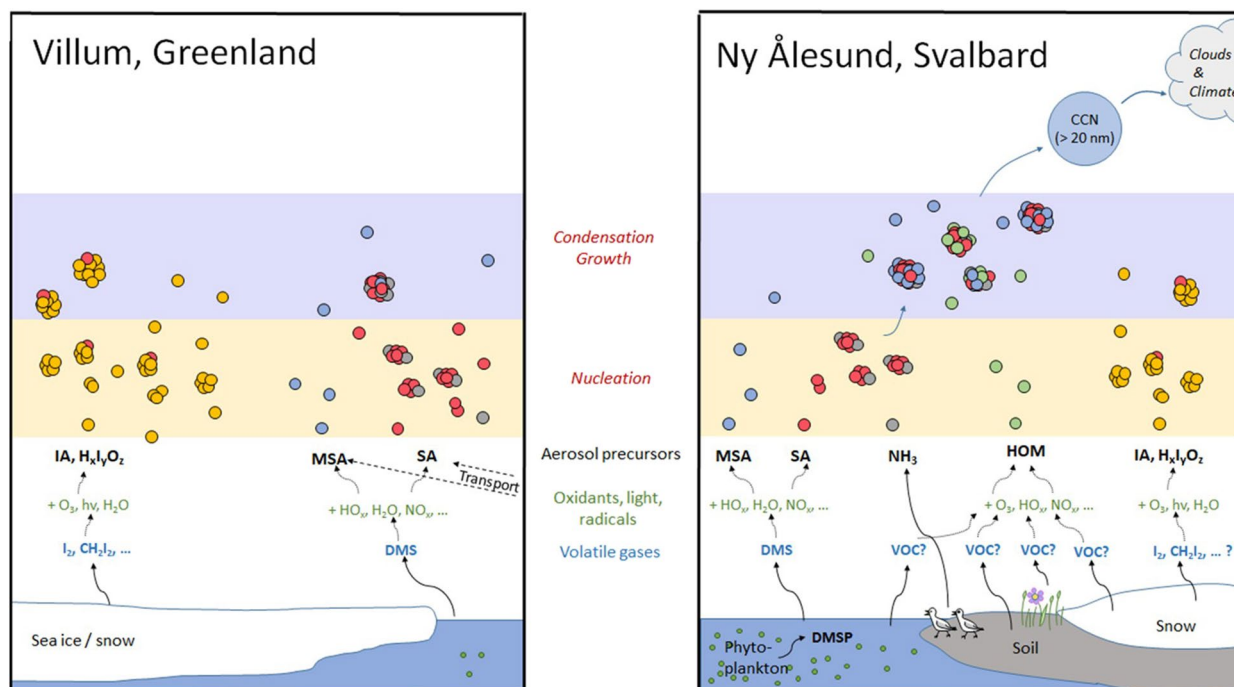
Figure 4. Observed mechanisms of Arctic secondary aerosol formation involving iodine compounds (especially iodic acid, IA), methane sulfonic acid (MSA), sulfuric acid (SA), ammonia (NH_3), and highly oxygenated organic molecules (HOM). Nucleation and growth mechanisms vary spatially and temporally. The main mechanisms observed at two sites are shown in the figure.

newly formed particles are able to act as CCN. At the Zeppelin Observatory (480 m a.s.l. above Ny-Ålesund), activation of nucleated particles into droplets of low-level liquid clouds was observed once these particles had grown to sizes larger than about 20 nm (Figure S8). Activation of Aitken mode aerosol particles as small as 20 nm into cloud elements was shown to occur on a regular basis at Zeppelin, especially in the absence of accumulation mode particles and when the particle number size distribution was dominated by recent NPF (Karlsson et al., 2020). Based on these analyses, we speculate that atmospheric NPF observed at Ny-Ålesund, despite a rather slow consequent growth to Aitken mode size aerosol, may also contribute to the regional CCN budget.

At Villum, the lower concentration of SA and MSA compared to Ny-Ålesund can be explained by the extensive presence of sea ice in the region around Villum, limiting the formation of DMSP producing phytoplankton blooms and preventing gas exchange between the ocean and atmosphere (Figure S9). In our study, at Villum, IA alone seems insufficient to grow particles effectively into CCN size regimes. However, in other parts of ice-covered oceans with stronger iodine sources growth to CCN sizes can occur as recently shown by Baccarini et al. (2020). IA-containing particles might also serve as seeds for SA, MSA or organic matter condensation if advected over areas with stronger DMS or VOC emissions. Thus, iodine emissions from sea ice might still be important for Arctic CCN budgets close to the sea ice edge and in regions with non-consolidated ice. Furthermore, in other parts of ice-covered oceans, where iodine emissions and thus IA concentrations are higher, the iodine-mediated formation and aerosol growth to CCN size particles will be more effective. Iodine-containing CCN-sized particles have been detected in measurements done in the Greenland Sea (Allan et al., 2015).

4. Conclusions and Implications for the Changing Arctic Environment

Our novel measurement techniques enabled the observation of the very first steps of nucleation and growth at a molecular level, complementing the current understanding of NPF in the Arctic (Baccarini et al., 2020; Dall'Osto et al., 2017, 2018, 2019). Our observations show great disparity in particle precursor vapor concen-

trations and NPF events between the two Arctic locations with divergent environmental settings (Figure 4, Figure S1). Over the open water surrounding Ny-Ålesund, we observed that ion-induced nucleation of SA and NH_3 is an important pathway for secondary aerosol formation during the Arctic spring, with nucleation rates being sensitive to both, SA and NH_3 concentration. These observations are in good agreement with the study of H. Lee et al. (2020), showing that NPF is associated with enhanced DMS and NH_3 concentrations at the Zeppelin station, Svalbard. According to our observations, MSA and SA were critical for the particle growth in springtime. With high HOM concentrations during summertime, this compound class was likely to be involved in nucleation (Lehtipalo et al., 2018) and probably gave the dominant contribution to subsequent particle growth, especially because all the other low-volatility vapors had rather low concentrations. The region of sea ice-covered ocean surrounding Villum showed a much weaker particle growth throughout the measurement period. In springtime, we observed pure iodic acid nucleation at Villum, whereas in summertime, we observed weak SA-NH_3 nucleation.

Enhanced DMS emissions associated with sea ice loss and higher surface water temperatures have already been reported over the summertime Arctic Ocean (Galí et al., 2019; Li et al., 2019). Further sea ice loss might increase the productivity of pelagic phytoplankton (Ardyna et al., 2014; Renaut et al., 2018), and/or seawater-atmosphere exchange, which could lead to even higher atmospheric DMS concentrations in the future. In the regions dominated by sea ice, IA seems to be an important contributor to the nucleation and growth processes, although the newly formed particles seldom grow to CCN sizes where they become relevant for cloud formation, unless the air mass is transported over regions with strong emissions of DMS or gaseous precursors to SA. Thinning sea ice will likely lead to enhanced emissions of iodine due to more efficient transpassing of radiation and gases through the ice layer (Cuevas et al., 2018), causing elevated atmospheric IA concentrations. Those enhanced emissions will likely be a transient effect while the sea ice continues diminishing. Emissions of VOC are expected to increase with warming climate and lesser snow coverage, at least from peat and tundra vegetation (Lindwall et al., 2016) but possibly also from the Arctic Ocean (Mungall et al., 2017), which would be reflected in higher concentrations of HOM and accelerated secondary aerosol formation. Based on our results on mechanisms of aerosol formation, all these changes would lead to an increased production of new aerosol particles and their potential growth to CCN, thus affecting cloud microphysical properties in the summer Arctic atmosphere (Mahmood et al., 2019; Ridley et al., 2016). It remains, however, uncertain how, for example, phytoplankton will respond to other components of Arctic change (Hoppe et al., 2018) or how bird populations respond to global change and concomitant changes in the marine food web (Howard et al., 2018).

We have shown the process chain from the phytoplankton metabolite production to CCN-size aerosol formation, and confirmed the importance of oceanic DMS and NH_3 emissions as well as galactic cosmic radiation in Arctic secondary aerosol formation (Figure 4). Furthermore, we have illustrated the role of iodine and HOM emissions in this process. Definite predictions on how CCN concentrations and radiative forcing will respond to Arctic change cannot yet be made. Still our findings are critical for assessing the relevance of the famous, yet debated CLAW-hypothesis (Charlson et al., 1987; Quinn & Bates, 2011), which suggests a negative feedback of climate warming via enhanced phytoplankton productivity. The mechanistic understanding obtained here will help to improve large-scale models to shed more light on the pre-industrial, present and future aerosol state and on the magnitude of total radiative forcing associated with the inevitable Arctic warming and evanescence of sea ice.

Data Availability Statement

The data are available at Zenodo (https://doi.org/10.5281/zenodo.4292239).

References

Allan, J. D., Williams, P. I., Najera, J., Whitehead, J. D., Flynn, M. J., Taylor, J. W., et al. (2015). Iodine observed in new particle formation events in the Arctic atmosphere during ACCACIA. *Atmospheric Chemistry and Physics*, *15*, 5599–5609. https://doi.org/10.5194/acp-15-5599-2015

AMAP. (2017). *AMAP, 2017. Snow, water, ice and permafrost in the Arctic (SWIPA): Climate change and the cryosphere*. Arctic Monitoring and Assessment Programme (AMAP), 269.

Ardyna, M., Babin, M., Gosselin, M., Devred, E., Rainville, L., & Tremblay, J.-É. (2014). Recent Arctic Ocean sea ice loss triggers novel fall phytoplankton blooms. *Geophysical Research Letters*, *41*, 6207–6212. https://doi.org/10.1002/2014GL061047

Assmy, P., Fernández-Méndez, M., Duarte, P., Meyer, A., Randelhoff, A., Mundy, C. J., et al. (2017). Leads in Arctic pack ice enable early phytoplankton blooms below snow-covered sea ice. *Scientific Reports*, *7*, 40850. https://doi.org/10.1038/srep40850

Baccarini, A., Karlsson, L., Dommen, J., Duplessis, P., Vüllers, J., Brooks, I. M., et al. (2020). Frequent new particle formation over the high Arctic pack ice by enhanced iodine emissions. *Nature Communications*, *11*, 4924. https://doi.org/10.1038/s41467-020-18551-0

Berresheim, H., Elste, T., Tremmel, H. G., Allen, A. G., Hansson, H.-C., Rosman, K., et al. (2002). Gas-aerosol relationships of H2SO4, MSA, and OH: Observations in the coastal marine boundary layer at Mace Head, Ireland. *Journal of Geophysical Research*, *107*(D19), PAR 5-1-PAR 5-12. https://doi.org/10.1029/2000JD000229

Bianchi, F., Kurtén, T., Riva, M., Mohr, C., Rissanen, M. P., Roldin, P., et al. (2019). Highly oxygenated organic molecules (HOM) from gas-phase autoxidation involving peroxy radicals: A key contributor to atmospheric aerosol. *Chemical Reviews*, *119*, 3472–3509. https://doi.org/10.1021/acs.chemrev.8b00395

Callaghan, T. V., Johansson, M., Brown, R. D., Groisman, P. Ya., Labba, N., Radionov, V., et al. (2011). The changing face of Arctic snow cover: A synthesis of observed and projected changes. *Ambio*, *40*, 17–31. https://doi.org/10.1007/s13280-011-0212-y

Charlson, R. J., Lovelock, J. E., Andreae, M. O., & Warren, S. G. (1987). Oceanic phytoplankton, atmospheric sulfur, cloud albedo and climate. *Nature*, *326*(6114), 655–661. https://doi.org/10.1038/326655a0

Chen, Q., Sherwen, T., Evans, M., & Alexander, B. (2018). DMS oxidation and sulfur aerosol formation in the marine troposphere: A focus on reactive halogen and multiphase chemistry. *Atmospheric Chemistry and Physics*, *18*, 13617–13637. https://doi.org/10.5194/acp-18-13617-2018

Chen, L., Wang, J., Gao, Y., Xu, G., Yang, X., Lin, Q., & Zhang, Y. (2012). Latitudinal distributions of atmospheric MSA and MSA/nss-SO42− Ratios in summer over the high latitude regions of the Southern and Northern Hemispheres. *Journal of Geophysical Research*, *117*, D10306. https://doi.org/10.1029/2011JD016559

Croft, B., Wentworth, G. R., Martin, R. V., Leaitch, W. R., Murphy, J. G., Murphy, B. N., et al. (2016). Contribution of Arctic seabird-colony ammonia to atmospheric particles and cloud-albedo radiative effect. *Nature Communications*, *7*, 1–10. https://doi.org/10.1038/ncomms13444

Cuevas, C. A., Maffezzoli, N., Corella, J. P., Spolaor, A., Vallelonga, P., Kjær, H. A., et al. (2018). Rapid increase in atmospheric iodine levels in the North Atlantic since the mid-20th century. *Nature Communications*, *9*, 1–6. https://doi.org/10.1038/s41467-018-03756-1

Dall'Osto, M., Beddows, D. C. S., Tunved, P., Harrison, R. M., Lupi, A., Vitale, V., et al. (2019). Simultaneous measurements of aerosol size distributions at three sites in the European high Arctic. *Atmospheric Chemistry and Physics*, *19*, 7377–7395. https://doi.org/10.5194/acp-19-7377-2019

Dall'Osto, M., Beddows, D. C. S., Tunved, P., Krejci, R., Ström, J., Hansson, H. C., et al. (2017). Arctic sea ice melt leads to atmospheric new particle formation. *Scientific Reports*, *7*, 1–10. https://doi.org/10.1038/s41598-017-03328-1

Dall'Osto, M., Geels, C., Beddows, D. C. S., Boertmann, D., Lange, R., Nøjgaard, J. K., et al. (2018). Regions of open water and melting sea ice drive new particle formation in North East Greenland. *Scientific Reports*, *8*, 1–10. https://doi.org/10.1038/s41598-018-24426-8

Dawson, M. L., Varner, M. E., Perraud, V., Ezell, M. J., Gerber, R. B., & Finlayson-Pitts, B. J. (2012). Simplified mechanism for new particle formation from methane sulfonic acid, amines, and water via experiments and ab initio calculations. *Proceedings of the National Academy of Sciences*, *109*(46), 18719–18724. https://doi.org/10.1073/pnas.1211878109

Dunne, E. M., Gordon, H., Kürten, A., Almeida, J., Duplissy, J., Williamson, C., et al. (2016). Global atmospheric particle formation from CERN CLOUD measurements. *Science*, *354*, 1119–1124. https://doi.org/10.1126/science.aaf2649

Ehn, M., Thornton, J. A., Kleist, E., Sipilä, M., Junninen, H., Pullinen, I., et al. (2014). A large source of low-volatility secondary organic aerosol. *Nature*, *506*, 476–479. https://doi.org/10.1038/nature13032

Galí, M., Devred, E., Babin, M., & Levasseur, M. (2019). Decadal increase in Arctic dimethylsulfide emission. *Proceedings of the National Academy of Sciences*, *116*, 19311–19317. https://doi.org/10.1073/pnas.1904378116

Giamarelou, M., Eleftheriadis, K., Nyeki, S., Tunved, P., Torseth, K., & Biskos, G. (2016). Indirect evidence of the composition of nucleation mode atmospheric particles in the high Arctic. *Journal of Geophysical Research: Atmospheres*, *121*, 965–975. https://doi.org/10.1002/2015JD023646

Gordon, H., Kirkby, J., Baltensperger, U., Bianchi, F., Breitenlechner, M., Curtius, J., et al. (2017). Causes and importance of new particle formation in the present-day and preindustrial atmospheres. *Journal of Geophysical Research: Atmosphere*, *122*, 8739–8760. https://doi.org/10.1002/2017JD026844

Halonen, R., Zapadinsky, E., Kurtén, T., Vehkamäki, H., & Reischl, B. (2019). Rate enhancement in collisions of sulfuric acid molecules due to long-range intermolecular forces. *Atmospheric Chemistry and Physics*, *19*, 13355–13366. https://doi.org/10.5194/acp-19-13355-2019

Hegseth, E. N., Assmy, P., Wiktor, J. M., Wiktor, J., Kristiansen, S., Leu, E., et al. (2019). *Phytoplankton seasonal dynamics in Kongsfjorden, Svalbard and the adjacent shelf*. Svalbard: The Ecosystem of Kongsfjorden. https://doi.org/10.1007/978-3-319-46425-1_6173227

Hodshire, A. L., Campuzano-Jost, P., Kodros, J. K., Croft, B., Nault, B. A., Schroder, J. C., et al. (2019). The potential role of methane sulfonic acid (MSA) in aerosol formation and growth and the associated radiative forcings. *Atmospheric Chemistry and Physics*, *19*, 3137–3160. https://doi.org/10.5194/acp-19-3137-2019

Hoppe, C. J. M., Wolf, K. K. E., Schuback, N., Tortell, P. D., & Rost, B. (2018). Compensation of ocean acidification effects in Arctic phytoplankton assemblages. *Nature Climate Change*, *8*, 529–533. https://doi.org/10.1038/s41558-018-0142-9

Howard, C., Stephens, P. A., Tobias, J. A., Sheard, C., Butchart, S. H. M., & Willis, S. G. (2018). Flight range, fuel load and the impact of climate change on the journeys of migrant birds. *Proceedings of the Royal Society B: Biological Sciences*, *285*, 20172329. https://doi.org/10.1098/rspb.2017.2329

Hudson, J. G., & Noble, S. (2014). CCN and vertical velocity influences on droplet concentrations and supersaturations in clean and polluted stratus clouds. *Journal of the Atmospheric Sciences*, *71*, 312–331. https://doi.org/10.1175/JAS-D-13-086.1

Jokinen, T., Sipilä, M., Junninen, H., Ehn, M., Lönn, G., Hakala, J., et al. (2012). Atmospheric sulfuric acid and neutral cluster measurements using CI-APi-TOF. *Atmospheric Chemistry and Physics*, *12*, 4117–4125. https://doi.org/10.5194/acp-12-4117-2012

Jokinen, T., Sipilä, M., Kontkanen, J., Vakkari, V., Tisler, P., Duplissy, E. M., et al. (2018). Ion-induced sulfuric acid–ammonia nucleation drives particle formation in coastal Antarctica. *Science Advances*, *4*, eaat9744. https://doi.org/10.1126/sciadv.aat9744

Junninen, H., Ehn, M., Petäjä, T., Luosujärvi, L., Kotiaho, T., Kostiainen, R., et al. (2010). A high-resolution mass spectrometer to measure atmospheric ion composition. *Atmospheric Measurement Techniques*, *3*, 1039–1053. https://doi.org/10.5194/amt-3-1039-2010

Karlsson, L., Krejci, R., Koike, M., Ebell, K., & Zieger, P. (2020). The role of nanoparticles in Arctic cloud formation. *Atmospheric Chemistry and Physics Discussions*, 1–30. https://doi.org/10.5194/acp-2020-417

Kerminen, V. M., Paramonov, M., Anttila, T., Riipinen, I., Fountoukis, C., Korhonen, H., et al. (2012). Cloud condensation nuclei production associated with atmospheric nucleation: A synthesis based on existing literature and new results. *Atmospheric Chemistry and Physics*, *12*, 12037–12059. https://doi.org/10.5194/acp-12-12037-2012

Kirkby, J., Curtius, J., Almeida, J., Dunne, E., Duplissy, J., Ehrhart, S., et al. (2011). Role of sulfuric acid, ammonia and galactic cosmic rays in atmospheric aerosol nucleation. *Nature*, *476*, 429–433. https://doi.org/10.1038/nature10343

Kirkby, J., Duplissy, J., Sengupta, K., Frege, C., Gordon, H., Williamson, C., et al. (2016). Ion-induced nucleation of pure biogenic particles. *Nature*, *533*, 521–526. https://doi.org/10.1038/nature17953

Lange, R., Dall'Osto, M., Skov, H., Nøjgaard, J. K., Nielsen, I. E., Beddows, D. C. S., et al. (2018). Characterization of distinct Arctic aerosol accumulation modes and their sources. *Atmospheric Environment*, *183*, 1–10. https://doi.org/10.1016/j.atmosenv.2018.03.060

Lee, S.-H., Gordon, H., Yu, H., Lehtipalo, K., Haley, R., Li, Y., & Zhang, R. (2019). New particle formation in the atmosphere: From molecular clusters to global climate. *Journal of Geophysical Research: Atmosphere*, *124*, 7098–7146. https://doi.org/10.1029/2018JD029356

Lee, H., Lee, K., Lunder, C. R., Krejci, R., Aas, W., Park, J., et al. (2020). Atmospheric new particle formation characteristics in the Arctic as measured at Mount Zeppelin, Svalbard, from 2016 to 2018. *Atmospheric Chemistry and Physics Discussions*, 1–28. https://doi.org/10.5194/acp-2020-390

Lehtipalo, K., Yan, C., Dada, L., Bianchi, F., Xiao, M., Wagner, R., et al. (2018). Multicomponent new particle formation from sulfuric acid, ammonia, and biogenic vapors. *Science Advances*, *4*, eaau5363. https://doi.org/10.1126/sciadv.aau5363

Levasseur, M. (2013). Impact of Arctic meltdown on the microbial cycling of sulfur. *Nature Geoscience*, *6*, 691–700. https://doi.org/10.1038/ngeo1910

Li, C. X., Wang, B. D., Wang, Z. C., Li, J., Yang, G. P., Chen, J. F., et al. (2019). Spatial and interannual variability in distributions and cycling of summer biogenic sulfur in the Bering Sea. *Geophysical Research Letters*, *46*, 4816–4825. https://doi.org/10.1029/2018GL080446

Lindwall, F., Schollert, M., Michelsen, A., Blok, D., & Rinnan, R. (2016). Fourfold higher tundra volatile emissions due to arctic summer warming. *Journal of Geophysical Research: Biogeosciences*, *121*, 895–902. https://doi.org/10.1002/2015JG003295

Mahmood, R., Salzen, K. von, Norman, A. L., Galí, M., & Levasseur, M. (2019). Sensitivity of Arctic sulfate aerosol and clouds to changes in future surface seawater dimethylsulfide concentrations. *Atmospheric Chemistry and Physics*, *19*, 6419–6435. https://doi.org/10.5194/acp-19-6419-2019

Manninen, H. E., Petäjä, T., Asmi, E., Riipinen, I., Mikkilä, J., Hõrrak, U., et al. (2009). Long-term field measurements of charged and neutral clusters using Neutral cluster and Air Ion Spectrometer (NAIS). *Boreal Environment Research*, *14*, 591–605.

Meier, W. N., Hovelsrud, G. K., Oort, B. E. H. van, Key, J. R., Kovacs, K. M., Michel, C., et al. (2014). Arctic sea ice in transformation: A review of recent observed changes and impacts on biology and human activity. *Reviews of Geophysics*, *52*, 185–217. https://doi.org/10.1002/2013RG000431

Mirme, S., & Mirme, A. (2013). The mathematical principles and design of the NAIS – A spectrometer for the measurement of cluster ion and nanometer aerosol size distributions. *Atmospheric Measurement Techniques*, *6*, 1061–1071. https://doi.org/10.5194/amt-6-1061-2013

Moore, R. H., Karydis, V. A., Capps, S. L., Lathem, T. L., & Nenes, A. (2013). Droplet number uncertainties associated with CCN: An assessment using observations and a global model adjoint. *Atmospheric Chemistry and Physics*, *13*, 4235–4251. https://doi.org/10.5194/acp-13-4235-2013

Mungall, E. L., Abbatt, J. P. D., Wentzell, J. J. B., Lee, A. K. Y., Thomas, J. L., Blais, M., et al. (2017). Microlayer source of oxygenated volatile organic compounds in the summertime marine Arctic boundary layer. *Proceedings of the National Academy of Sciences*, *114*, 6203–6208. https://doi.org/10.1073/pnas.1620571114

Nguyen, Q. T., Glasius, M., Sørensen, L. L., Jensen, B., Skov, H., Birmili, W., et al. (2016). Seasonal variation of atmospheric particle number concentrations, new particle formation and atmospheric oxidation capacity at the high Arctic site Villum Research Station, Station Nord. *Atmospheric Chemistry and Physics*, *16*, 11319–11336. https://doi.org/10.5194/acp-16-11319-2016

Nielsen, I. E., Skov, H., Massling, A., Eriksson, A. C., Dall'Osto, M., Junninen, H., et al. (2019). Biogenic and anthropogenic sources of aerosols at the High Arctic site Villum Research Station. *Atmospheric Chemistry and Physics*, *19*, 10239–10256. https://doi.org/10.5194/acp-19-10239-2019

Nieminen, T., Lehtinen, K. E. J., & Kulmala, M. (2010). Sub-10 nm particle growth by vapor condensation – Effects of vapor molecule size and particle thermal speed. *Atmospheric Chemistry and Physics*, *10*, 9773–9779. https://doi.org/10.5194/acp-10-9773-2010

Pozzoli, L., Bey, I., Rast, S., Schultz, M. G., Stier, P., & Feichter, J. (2008). Trace gas and aerosol interactions in the fully coupled model of aerosol-chemistry-climate ECHAM5-HAMMOZ: 2. Impact of heterogeneous chemistry on the global aerosol distributions. *Journal of Geophysical Research*, *113*. https://doi.org/10.1029/2007JD009008

Quinn, P. K., & Bates, T. S. (2011). The case against climate regulation via oceanic phytoplankton sulfur emissions. *Nature*, *480*, 51–56. https://doi.org/10.1038/nature10580

Raso, A. R. W., Custard, K. D., May, N. W., Tanner, D., Newburn, M. K., Walker, L., et al. (2017). Active molecular iodine photochemistry in the Arctic. *Proceedings of the National Academy of Sciences*, *114*, 10053–10058. https://doi.org/10.1073/pnas.1702803114

Renaut, S., Devred, E., & Babin, M. (2018). Northward expansion and intensification of phytoplankton growth during the early ice-free season in Arctic. *Geophysical Research Letters*, *45*, 10590–10598. https://doi.org/10.1029/2018GL078995

Riccobono, F., Schobesberger, S., Scott, C. E., Dommen, J., Ortega, I. K., Rondo, L., et al. (2014). Oxidation products of biogenic emissions contribute to nucleation of atmospheric particles. *Science*, *344*, 717–721. https://doi.org/10.1126/science.1243527

Ridley, J. K., Ringer, M. A., & Sheward, R. M. (2016). The transformation of Arctic clouds with warming. *Climatic Change*, *139*, 325–337. https://doi.org/10.1007/s10584-016-1772-4

Saiz-Lopez, A., Blaszczak-Boxe, C. S., & Carpenter, L. J. (2015). A mechanism for biologically induced iodine emissions from sea ice. *Atmospheric Chemistry and Physics*, *15*, 9731–9746. https://doi.org/10.5194/acp-15-9731-2015

Sipilä, M., Sarnela, N., Jokinen, T., Henschel, H., Junninen, H., Kontkanen, J., et al. (2016). Molecular-scale evidence of aerosol particle formation via sequential addition of HIO3. *Nature*, *537*, 532–534. https://doi.org/10.1038/nature19314

Stefels, J., Steinke, M., Turner, S., Malin, G., & Belviso, S. (2007). Environmental constraints on the production and removal of the climatically active gas dimethyl sulphoxide (DMS) and implications for ecosystem modeling. *Biogeochemistry*, *83*, 245–275. https://doi.org/10.1007/s10533-007-9091-5

Vanhanen, J., Mikkilä, J., Lehtipalo, K., Sipilä, M., Manninen, H. E., Siivola, E., et al. (2011). Particle size magnifier for Nano-CN detection. *Aerosol Science and Technology*, *45*, 533–542. https://doi.org/10.1080/02786826.2010.547889

Wang, S. C., & Flagan, R. C. (1990). Scanning electrical mobility spectrometer. *Aerosol Science and Technology*, *13*(2), 230–240. https://doi.org/10.1080/02786829008959441

Zhao, X., Liu, Y., Yu, F., & Heidinger, A. K. (2018). Using long-term satellite observations to identify sensitive regimes and active regions of aerosol indirect effects for liquid clouds over global oceans. *Journal of Geophysical Research: Atmosphere*, *123*, 457–472. https://doi.org/10.1002/2017JD027187

References From the Supporting Information

Buenrostro Mazon, S., Riipinen, I., Schultz, D. M., Valtanen, M., Maso, M. D., Sogacheva, L., et al. (2009). Classifying previously undefined days from eleven years of aerosol-particle-size distribution data from the SMEAR II station, Hyytiälä, Finland. *Atmospheric Chemistry and Physics*, *9*, 667–676. https://doi.org/10.5194/acp-9-667-2009

Dada, L., Chellapermal, R., Buenrostro Mazon, S., Paasonen, P., Lampilahti, J., Manninen, H. E., et al. (2018). Refined classification and characterization of atmospheric new-particle formation events using air ions. *Atmospheric Chemistry and Physics*, *18*, 17883–17893. https://doi.org/10.5194/acp-18-17883-2018

Eisele, F. L., & Tanner, D. J. (1993). Measurement of the gas phase concentration of H_2SO_4 and methane sulfonic acid and estimates of H_2SO_4 production and loss in the atmosphere. *Journal of Geophysical Research*, *98*(D5), 9001–9010. https://doi.org/10.1029/93JD00031

Hyttinen, N., Kupiainen-Määttä, O., Rissanen, M. P., Muuronen, M., Ehn, M., & Kurtén, T. (2015). Modeling the charging of highly oxidized cyclohexene ozonolysis products using nitrate-based chemical ionization. *The Journal of Physical Chemistry A*, *119*, 6339–6345. https://doi.org/10.1021/acs.jpca.5b01818

Kulmala, M., Petäjä, T., Nieminen, T., Sipilä, M., Manninen, H. E., Lehtipalo, K., et al. (2012). Measurement of the nucleation of atmospheric aerosol particles. *Nature Protocols*, *7*, 1651–1667. https://doi.org/10.1038/nprot.2012.091

Kürten, A., Rondo, L., Ehrhart, S., & Curtius, J. (2012). Calibration of a chemical ionization mass spectrometer for the measurement of gaseous sulfuric acid. *The Journal of Physical Chemistry A*, *116*, 6375–6386. https://doi.org/10.1021/jp212123n

Manninen, H. E., Nieminen, T., Asmi, E., Gagné, S., Häkkinen, S., Lehtipalo, K., et al. (2010). EUCAARI ion spectrometer measurements at 12 European sites – Analysis of new particle formation events. *Atmospheric Chemistry and Physics*, *10*, 7907–7927. https://doi.org/10.5194/acp-10-7907-2010

Paatero, P., & Tapper, U. (1994). Positive matrix factorization: A non-negative factor model with optimal utilization of error estimates of data values. *Environmetrics*, *5*(2), 111–126. https://doi.org/10.1002/env.3170050203

Seinfeld, J. H., & Pandis, S. N. (2016). *Atmospheric chemistry and physics: From air pollution to climate change*. John Wiley & Sons.

Stolzenburg, D., Simon, M., Ranjithkumar, A., Kürten, A., Lehtipalo, K., Gordon, H., et al. (2019). Enhanced growth rate of atmospheric particles from sulfuric acid. *Atmospheric Chemistry and Physics Discussions*, 1–17. https://doi.org/10.5194/acp-2019-755

Tammet, H. (1998). Reduction of air ion mobility to standard conditions. *Journal of Geophysical Research*, *103*(D12), 13933–13937. https://doi.org/10.1029/97JD01429

Virkkula, A., Hirsikko, A., Vana, M., Aalto, P. P., Hillamo, R., & Kulmala, M. (2007). Charged particle size distributions and analysis of particle formation events at the Finnish Antarctic research station Aboa. *Boreal Environment Research*, *12*, 397–408.

Zhang, Y., Peräkylä, O., Yan, C., Heikkinen, L., Äijälä, M., Daellenbach, K. R., et al. (2019). A novel approach for simple statistical analysis of high-resolution mass spectra. *Atmospheric Measurement Techniques*, *12*, 3761–3776. https://doi.org/10.5194/amt-12-3761-2019